

SUPPLEMENTAL INFORMATION

Title: Pseudotemporal ordering of single cells reveals metabolic control of postnatal beta-cell proliferation

Inventory:

I. Supplemental Data

Figure S1, Related to Figure 1

Figure S2, Related to Figure 2

Figure S3, Related to Figure 2

Figure S4, Related to Figure 3

Figure S5, Related to Figure 5

Figure S6, Related to Figure 6

Figure S7, Related to Figure 7

Table S1, Related to Figure 1

Table S2, Related to Figure 2

Table S3, Related to Figure S2

Table S4, Related to Figure 3

Table S5, Related to Figure 6

Table S6, Related to Figure 6 and Figure S6

Table S7, Related to Figure 7

I. Supplemental Data

Supplemental Figures

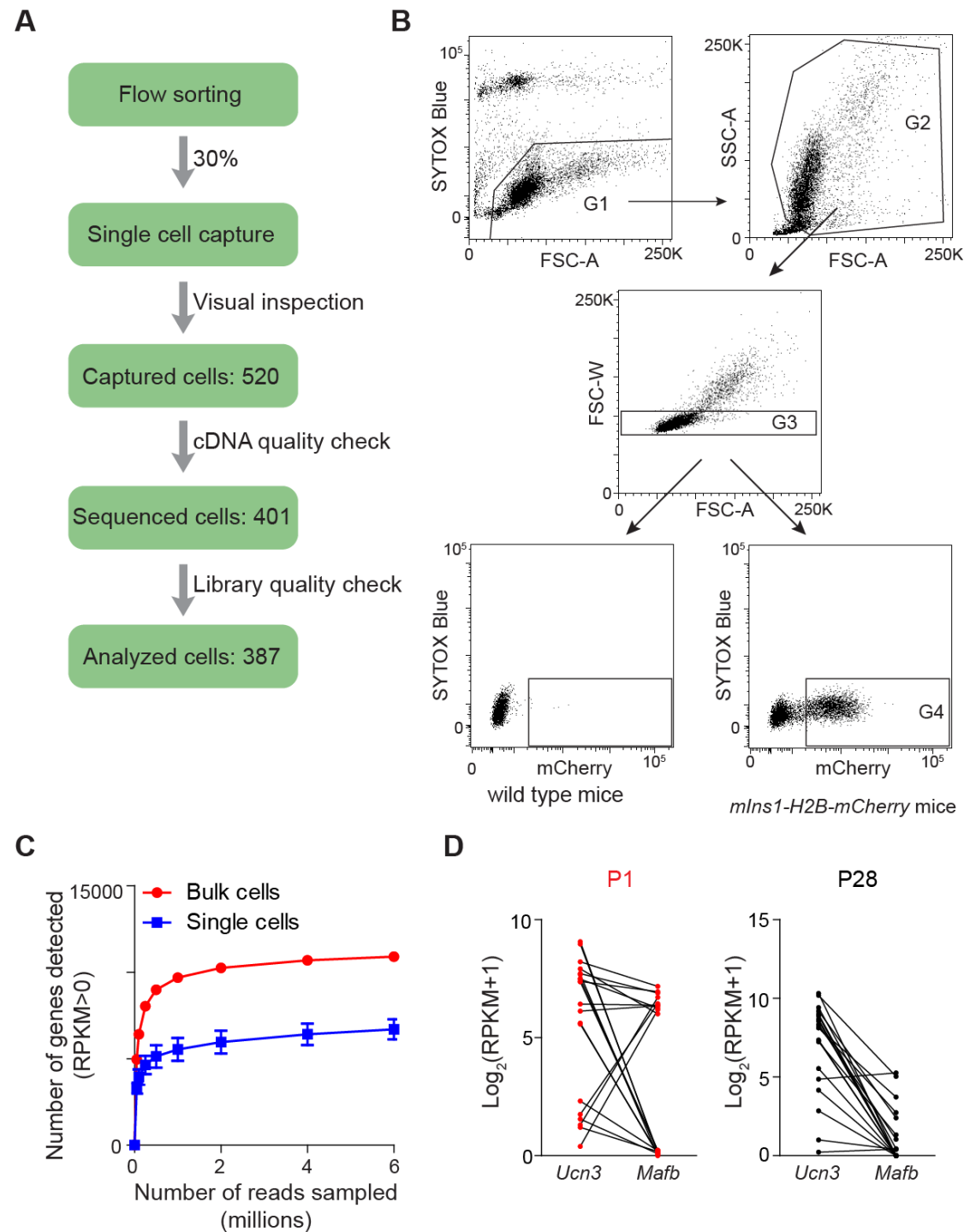


Figure S1. Quality control criteria used to generate and identify reliable single-cell libraries.

Related to Figure 1.

A. Schematic showing criteria used to identify reliable single-cell libraries. **B.** FACS strategy for isolating single, live beta-cells. Live cells were selected by gating for SYTOX Blue-negative cells (G1).

Beta-cells (G2) were gated by scatter (FSC-A vs. SSC-A) and single cells (G3) selected by gating out doublets using FSC-A vs. FSC-W. Cells expressing mCherry were sorted (G4). Sorting of beta-cells from wild type mice (bottom left) served as a negative control and are shown for comparison. **C.** Saturation curves for bulk and single cell libraries. Each point on the curve was generated by randomly selecting a number of raw reads from each sample library and then using the same alignment pipeline for all subsamples to call genes with RPKM > 0. Each point represents four replicate subsamplings. Error bars indicate SEM. **D.** Negative correlation of *Ucn3* and *Mafb* expression levels at an individual cell level. Each line represents the gene expression levels of *Ucn3* and *Mafb* of an individual beta-cell at P1 (red dots, left) and P28 (black dots, right). Beta-cells with highest (n=10) and lowest (n=10) expression of *Ucn3* were selected for analysis.

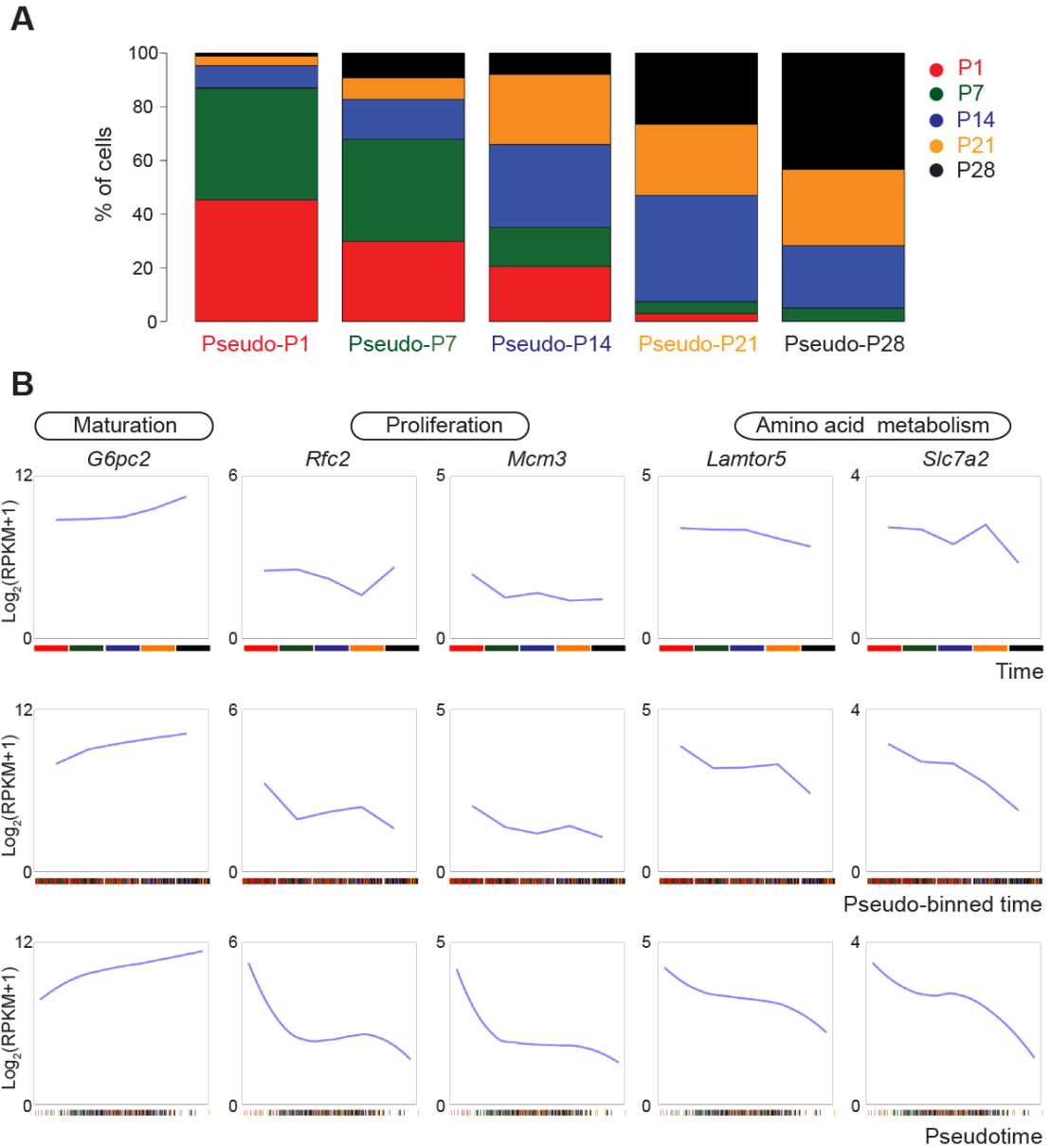


Figure S2. Beta-cell maturation-associated changes in gene expression with pseudotime compared to sample collection time. Related to Figure 2.

A. Stacked bar graph showing the percentage of cells from each of the collected time points contained in the pseudo-binned time-ordered groups. Collected time points are colored by postnatal (P) day collected (P1, red; P7, green; P14, blue; P21, orange; and P28, black). **B.** Expression profiles of selected genes ordered by time collected (top panels), pseudo-binned time (middle panels), or pseudotime (bottom panels). The trajectory of expression of *G6pc2*, a regulator of glycolysis, was similar in time-ordered and pseudotime-ordered cells, while different patterns of expression were observed for regulators of proliferation (*Rfc2* and *Mcm3*) and amino acid metabolism (*Lamtor5* and *Slc7a2*).

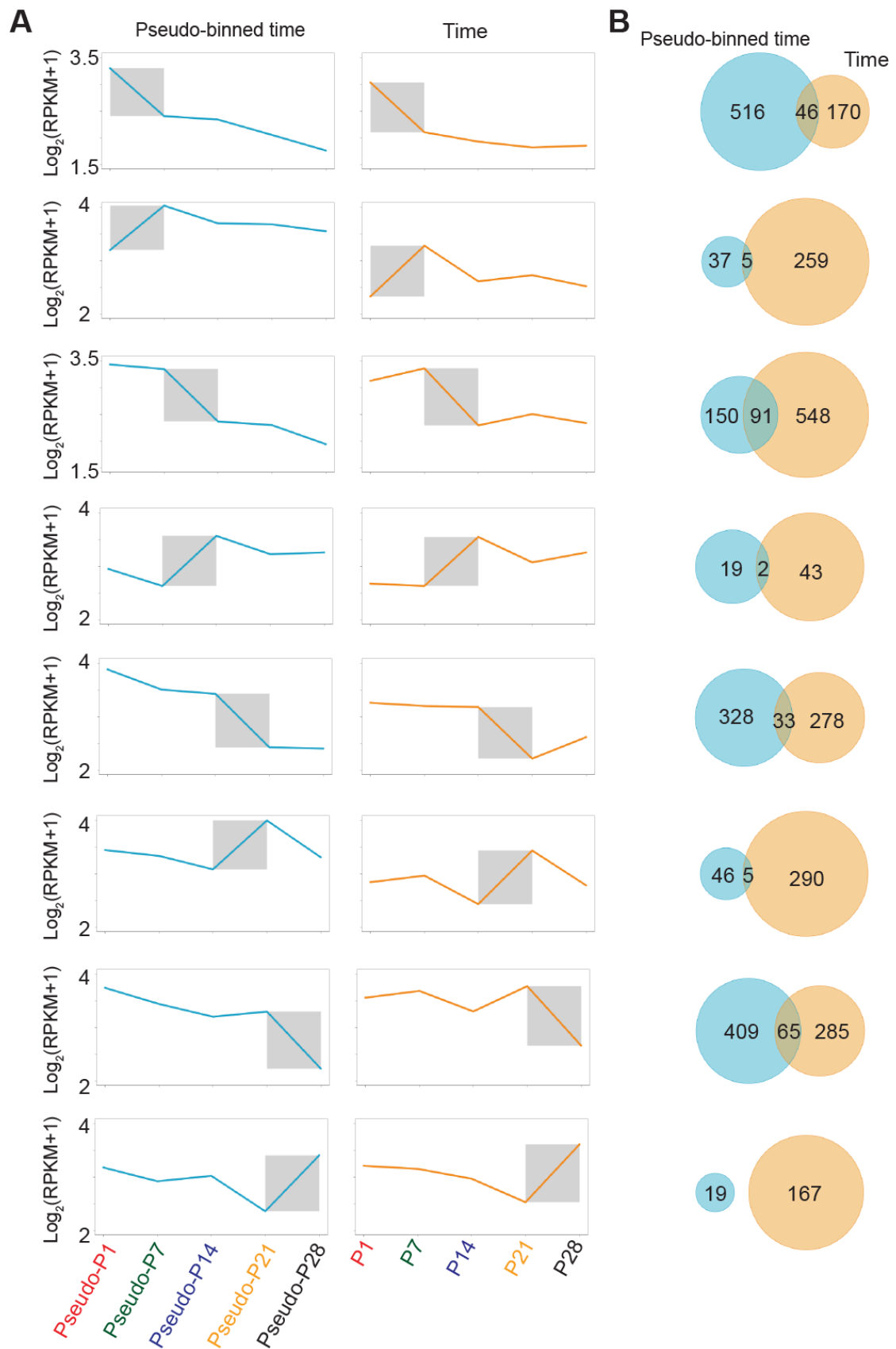


Figure S3. Comparison of pseudotime- and time-ordered gene expression patterns across the postnatal maturation time course. Related to Figure 2.

A. Gene expression patterns of cells ordered by pseudo-binned time (blue) or by time collected (orange) grouped by decreasing and increasing genes between two consecutive time points (grey boxes). **B.** Corresponding Venn diagram of the overlap between decreasing and increasing genes from pseudotime-ordered and time collected points.

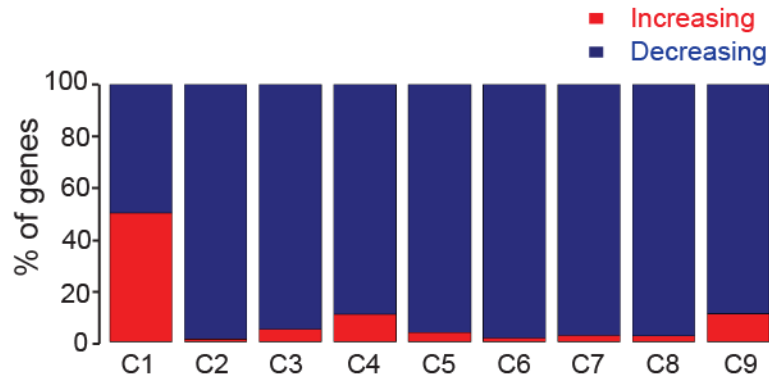


Figure S4. Clusters showing significant correlation with pseudotime-ordering comprised mostly downregulated genes. Related to Figure 3.

Percentage of genes increasing or decreasing during pseudotime in each of the nine clusters identified with *de novo* gene set discovery. Blue and red represent genes decreasing and increasing, respectively, with pseudotime.

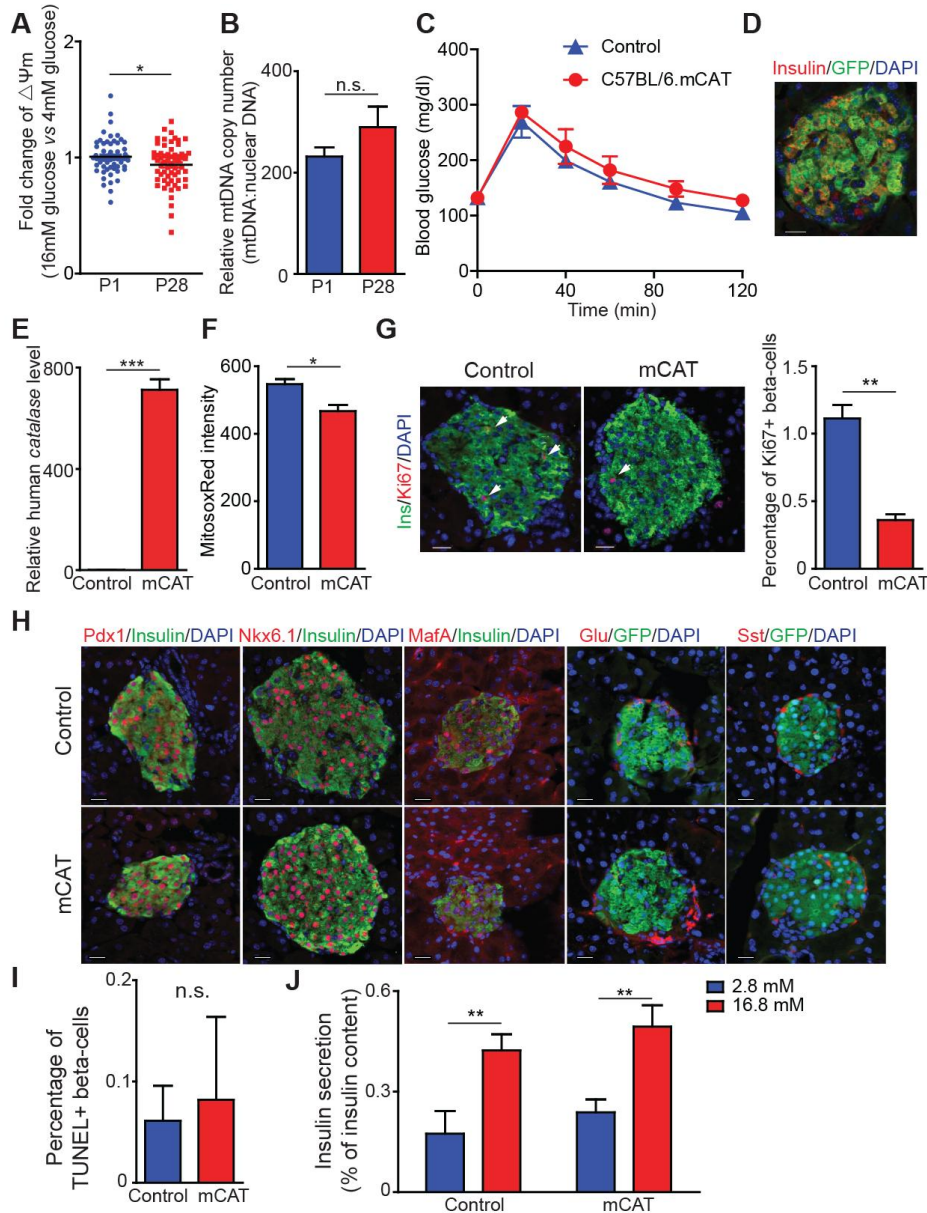


Figure S5. ROS levels affect beta-cell proliferation but not survival or insulin secretion. Related to Figure 5.

A. Islets from mice at P1 and P28 were cultured in TMRE and MitoTracker Green and sequentially exposed to 4 mM and 16 mM glucose. Shown is the fold change in $\Delta\Psi_m$ in 16 mM glucose over 4 mM glucose (n=67 beta-cells at P1, n=62 beta-cells at P28). Data are from three independent experiments.

B. Real-time PCR mtDNA/nDNA ratios of sorted beta-cells from P1 and P28 mice. Data shown as mean \pm SEM of four independent experiments.

C. 10-week-old mCAT mice on a C57BL/6 background not carrying a Cre recombinase transgene and C57BL/6 control mice were fasted for 6 hours and injected with 1.5 mg/kg glucose intraperitoneally before determining blood glucose levels (n=3 per group).

D, E. Generation of mice expressing mitochondrial-targeted catalase (mCAT) specifically in beta-cells. Representative immunofluorescence staining for insulin (red), GFP (to visualize YFP reporter expression; green), and DAPI (blue) showing efficient Cre recombinase-mediated recombination in beta-cells (**D**).

qRT-PCR of human *CAT* expression in mCAT and control (*RIP-Cre*) mice (**E**). Data shown as mean \pm SEM (n= 3-4 mice per group).

F. Quantification of islet mitochondrial

MitoxRed intensities as determined by FACS analysis of control (blue) and mCAT mice (red). Data shown as mean \pm SEM (n= 3 mice per group). **G.** Representative immunofluorescence staining for insulin (green), Ki67 (red), and DAPI (blue) is shown on the left. White arrows indicate Ins⁺Ki67⁺ cells. Quantification of the percentage of beta-cells expressing Ki67 in control (*RIP-Cre*) and mCAT mice at 6 weeks of age is shown on the right. Data shown as mean \pm SEM (n= 3 mice per group). **H.** Immunofluorescence staining for insulin, Pdx1, Nkx6.1, MafA, GFP, Glu, and Sst in control and mCAT mice. **I.** Quantification of the percentage of TUNEL⁺ beta-cells in control and mCAT mice. Data shown as mean \pm SEM (n= 3 mice per group). **J.** Glucose-stimulated insulin secretion in islets from control and mCAT mice. Data shown as mean \pm SEM (n= 4-5 mice per group). Scale bar represents 20 μ m. mtDNA, mitochondrial DNA; nDNA, nuclear DNA; Ins, Insulin; Glu, Glucagon; Sst, Somatostatin. * $P < 0.05$, ** $P < 0.01$, *** $P < 0.001$; n.s., not significant.

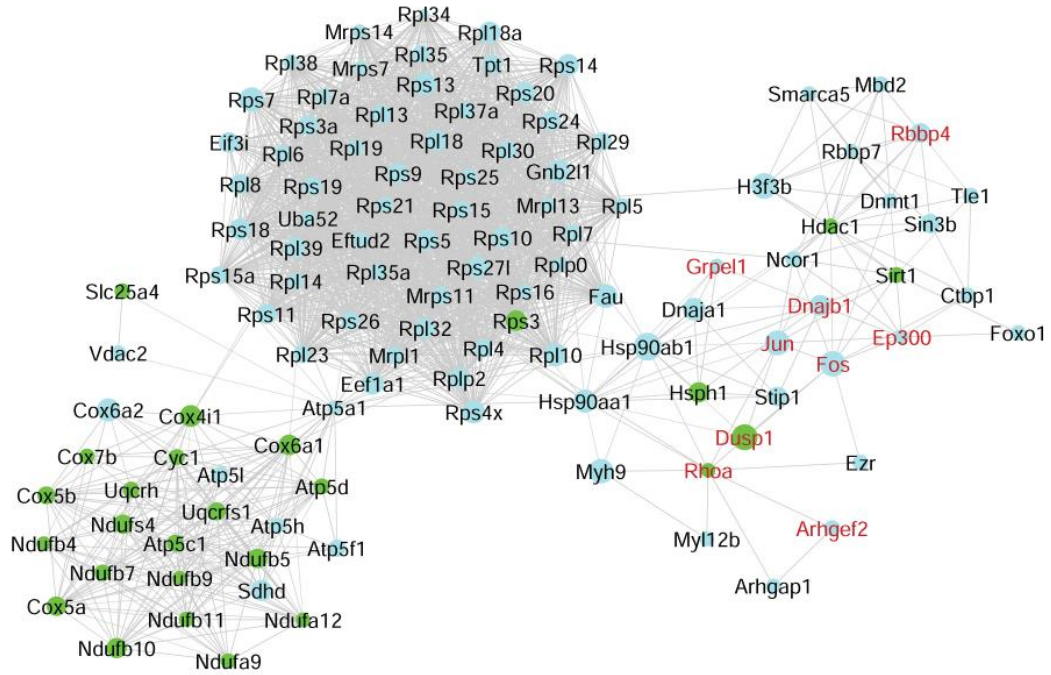


Figure S6. Network analysis reveals regulatory connection between oxidative phosphorylation-related genes and proliferation genes during beta-cell maturation. Related to Figure 6.

Network of interactomic connections of pseudotemporally regulated genes using oxidative phosphorylation-related genes as initial nodes of interest. Green nodes represent transcription factors while light blue nodes represent pseudotemporally-regulated genes. The size of the nodes is adjusted proportionally to the correlation coefficient of the gene expression level with pseudotime coordinates. Genes in red indicate those associated with proliferation.

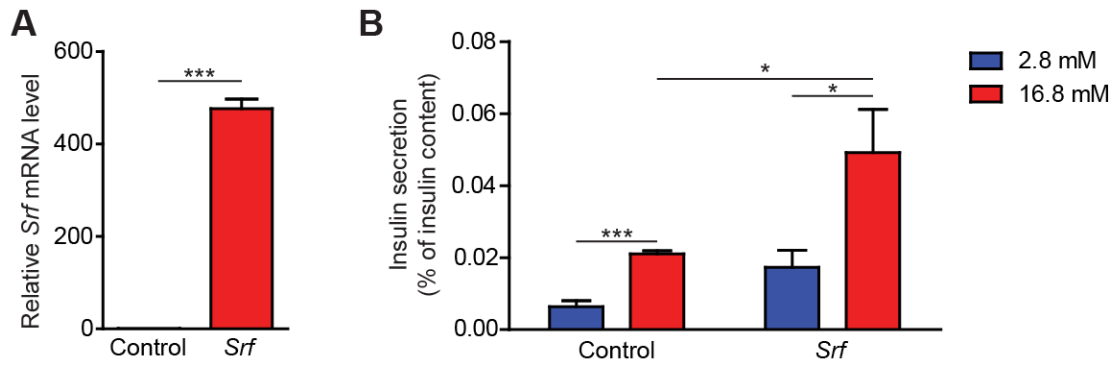


Figure S7. *Srf* overexpression in mouse islets enhances insulin secretion at high glucose. Related to Figure 7.

A. Quantitative RT-PCR analysis confirming induction of *Srf* transcripts after lentiviral transduction of islets from mice at P28. mRNA levels in islets transduced with a *GFP*-lentivirus were set as 1. Data shown as mean \pm SEM of three independent transduction experiments. **B.** Glucose stimulated insulin secretion was measured in control and *Srf*-overexpressing islets. Data shown as mean \pm SEM of six biological replicates. * $P < 0.05$, *** $P < 0.001$.

Supplemental Tables

Table S1: Summary of sequencing statistics, related to Figure 1.

(supplied as Excel file: Table S1. xlsx)

Table S2: Lists of the 1000 highest and 1000 lowest variable genes according to Median Absolute Deviation as well as genes used for data normalization, related to Figure 2. (A) List of the 1000 highest and 1000 lowest variable genes according to Median Absolute Deviation. (B) List of genes used for data normalization.

(supplied as Excel file: Table S2. xlsx)

Table S3: Lists of differentially expressed genes in consecutive pseudo-ordered and time-ordered samples, related to Figure S2. (A) Differentially expressed in consecutive pseudo-ordered samples. (B) Differentially expressed in consecutive time-ordered samples.

(supplied as Excel file: Table S3. xlsx)

Table S4: Information on significant annotated gene sets and *de novo* gene sets, related to Figure 3. (A) Significant annotated gene sets. (B) *De novo* gene sets. (C) List of genes in significant *de novo* gene sets.

(supplied as Excel file: Table S4. xlsx)

Table S5: Lists of genes and transcription factors significantly regulated during pseudotime and motifs enriched in active enhancers of these genes, related to Figure 6. (A) List of genes significantly regulated with pseudotime. (B) Motifs enriched in active enhancers of genes significantly regulated with pseudotime. (C) List of transcription factors (TFs) significantly regulated with pseudotime.

(supplied as Excel file: Table S5. xlsx)

Table S6: Lists of interest propagation scores in transcription factor-related network and oxidative phosphorylation-related network, related to Figure 6 and Figure S6. (A) Network-based interest propagation of transcription factor genes. (B) Network-based interest propagation of oxidative phosphorylation genes.

(supplied as Excel file: Table S6. xlsx)

Table S7: List of differentially expressed genes in *Srf*-overexpressing islets, related to Figure 7.

(supplied as Excel file: Table S7. xlsx)